

## Thermoelectric properties of fully hydrogenated graphene: Semi-classical Boltzmann theory

A. H. Reshak

Citation: *Journal of Applied Physics* **117**, 225104 (2015); doi: 10.1063/1.4922426

View online: <http://dx.doi.org/10.1063/1.4922426>

View Table of Contents: <http://scitation.aip.org/content/aip/journal/jap/117/22?ver=pdfcov>

Published by the [AIP Publishing](#)

---

### Articles you may be interested in

[Electronic and thermoelectric properties of InN studied using ab initio density functional theory and Boltzmann transport calculations](#)

*J. Appl. Phys.* **116**, 223706 (2014); 10.1063/1.4904086

[Thermoelectric properties of nanoporous three-dimensional graphene networks](#)

*Appl. Phys. Lett.* **105**, 033905 (2014); 10.1063/1.4883892

[Computational modeling and analysis of thermoelectric properties of nanoporous silicon](#)

*J. Appl. Phys.* **115**, 124316 (2014); 10.1063/1.4869734

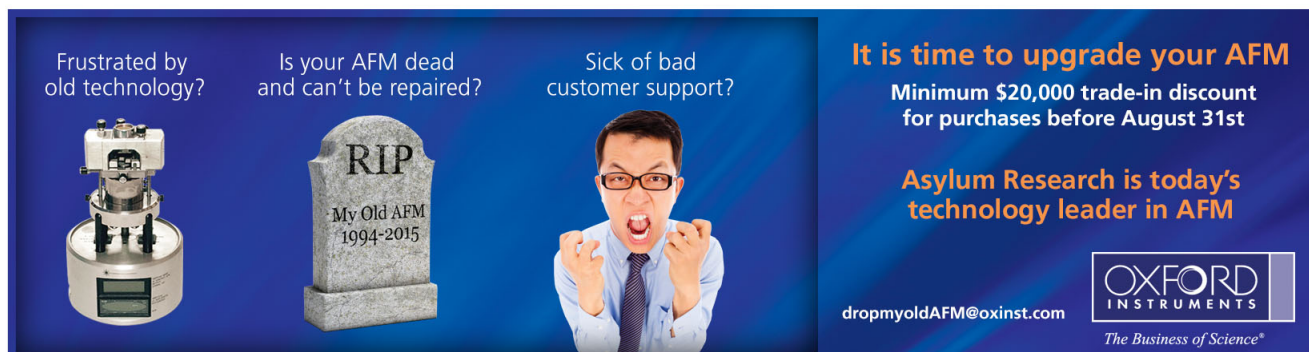
[Calculated thermoelectric properties of  \$\text{In}\_x\text{Ga}\_{1-x}\text{N}\$ ,  \$\text{In}\_x\text{Al}\_{1-x}\text{N}\$ , and  \$\text{Al}\_x\text{Ga}\_{1-x}\text{N}\$](#)

*J. Appl. Phys.* **113**, 183707 (2013); 10.1063/1.4804174

[Thermoelectric properties of bipolar diffusion effect on  \$\text{In}\_4\text{Se}\_3 - x\text{Te}\_x\$  compounds](#)

*Appl. Phys. Lett.* **97**, 152104 (2010); 10.1063/1.3493269

---



Frustrated by old technology? Is your AFM dead and can't be repaired? Sick of bad customer support?

**It is time to upgrade your AFM**  
Minimum \$20,000 trade-in discount for purchases before August 31st

Asylum Research is today's technology leader in AFM

dropmyoldAFM@oxinst.com

**OXFORD INSTRUMENTS**  
The Business of Science®

The advertisement features three panels: an old AFM, a tombstone for 'My Old AFM 1994-2015', and a frustrated man. The Oxford Instruments logo is in the bottom right corner.

# Thermoelectric properties of fully hydrogenated graphene: Semi-classical Boltzmann theory

A. H. Reshak<sup>1,2,a)</sup>

<sup>1</sup>New Technologies-Research Centre, University of West Bohemia, Univerzitni 8, 306 14 Pilsen, Czech Republic

<sup>2</sup>Center of Excellence Geopolymer and Green Technology, School of Material Engineering, University Malaysia Perlis, 01007 Kangar, Perlis, Malaysia

(Received 30 March 2015; accepted 1 June 2015; published online 11 June 2015)

Based on the calculated band structure, the electronic transport coefficients of chair-/boat-like graphane were evaluated by using the semi-classical Boltzmann theory and rigid band model. The maximum value of electrical conductivity for chair (boat)-like graphane of about  $1.4 (0.6) \times 10^{19} (\Omega\text{ms})^{-1}$  is achieved at 600 K. The charge carrier concentration and the electrical conductivity linearly increase with increasing the temperature in agreement with the experimental work for graphene. The investigated materials exhibit the highest value of Seebeck coefficient at 300 K. We should emphasize that in the chemical potential between  $\mp 0.125 \mu(\text{eV})$  the investigated materials exhibit minimum value of electronic thermal conductivity, therefore, maximum efficiency. As the temperature increases, the electronic thermal conductivity increases exponentially, in agreement with the experimental data of graphene. We also calculated the power factor of chair-/boat-like graphane at 300 and 600 K as a function of chemical potential between  $\mp 0.25 \mu(\text{eV})$ . © 2015 AIP Publishing LLC. [<http://dx.doi.org/10.1063/1.4922426>]

## I. INTRODUCTION

In the recent years, there is a focus on finding new energy resources and novel promising materials that can convert sun's energy into electricity to open a new direction for the ecologically friendly production of electrical energy. Thermoelectric materials as novel power generators can convert low grade heat into electricity, which appears to be a promising solution due to their friendly environment use and reasonable cost.<sup>1</sup> In order to investigate and enhance the thermoelectric properties, comprehensive research works on several materials were carried on<sup>2–11</sup> including graphene. Graphene has unique thermal and thermoelectric properties.<sup>12,13</sup> It reveals excellent electrical conductivity,<sup>14</sup> however, its exceedingly high thermal conductivity makes the graphene as poor contestant for thermoelectric applications.<sup>15</sup> On the other hand, different modifications can be applied to graphene's structure in order to reduce its thermal conductivity and thus increase the figure of merit. In order to improve the physical and chemical properties of graphene, adsorption of different chemical species (CO, N<sub>2</sub>O, NH<sub>3</sub>, and CO<sub>2</sub>) on its surface was investigated.<sup>16–19</sup> The previous literature exposed that organic electron donors,<sup>20</sup> acceptors,<sup>21</sup> or even DNA fragments<sup>22</sup> can induce considerable changes in the electronic structure of graphene, which make it suitable for new devices with optimized performances.

Several researchers modified graphene-based materials; Sluiter and Kawazoe<sup>23</sup> reported the existence of the hydrogenated graphene called graphane. Afterwards, Elias *et al.*<sup>24</sup>

synthesized the graphane by exposure of the graphene sheet to the hydrogen plasma. Since then, several new configurations were proposed for the newly discovered graphane, among the several configurations (stirrup, boat-1, boat-2, twisted-boat, chair), graphane is most stable in the chair-like configuration.<sup>23,25</sup> He *et al.*<sup>26</sup> reported that the hexagonal hydrocarbon ring is the most stable of the five graphane allotropes. Therefore, in this study we will focus on the comparison of the thermoelectric properties between the most stable configuration (chair-like) and one of the not so stable configuration (boat-like). Karlicky *et al.*<sup>27,28</sup> calculated the electronic structure and energy band gaps of graphane and stoichiometrically halogenated graphene derivatives (fluorographene and other analogous graphene halides) using the hybrid functional with localized orbital basis sets. Ni *et al.*<sup>29</sup> studied the thermoelectric property of graphane strips by using density functional theory (DFT) calculations combined with the non-equilibrium Green's function method. They reported that figure of merit (*ZT*) can be remarkably enhanced five times by randomly introducing hydrogen vacancies to the graphene nanoribbon derivatives armchair graphane nanoribbons.

To investigate the thermoelectric properties of chair-like and boat-like graphane, we think that it is timely to perform first-principles calculations using the state-of-the-art full-potential augmented plane wave plus local orbitals approach (FP-LAPW + lo) based on the density functional theory and the semi-classical Boltzmann theory as implemented in the BoltzTraP code.<sup>30</sup> We should emphasize that we are not aware of any theoretical or experiment work on the transport properties of these materials. This motivated us to calculate the thermoelectric properties of chair-like and boat-like graphane. Future experimental work will help testify our calculated results.

<sup>a)</sup>Author to whom correspondence should be addressed. Electronic mail: [maalidph@yahoo.co.uk](mailto:maalidph@yahoo.co.uk)

## II. DETAILS OF CALCULATION

The chair-like graphane has  $P-3m1$  (trigonal) space group, while the boat-like graphane has  $Pmnm$  (orthorhombic) space group. The crystal structure of both configurations is illustrated in Fig. 1. The state-of-the-art FPLAPW + lo method in a scalar relativistic version as embodied in the WIEN2k code<sup>31</sup> was used. Using the Perdew-Becke-Ernzerhof (PBE) generalized gradient approximation (GGA-PBE),<sup>32</sup> we have optimized the structure by minimization of the forces (1 mRy/au) acting on the atoms. From the relaxed geometry, the electronic structure and various spectroscopic features can be calculated and compared with experimental data. Once the forces are minimized in this construction one can then find the self-consistent density at these positions by turning off the relaxations and driving the system to self-consistency. To solve the exchange correlation potential, we have used Ceperley-Alder (CA) local density approximation (LDA)<sup>33</sup> and GGA-PBE, which are based on exchange-correlation energy optimization to calculate the total energy. In addition, to avoid LDA and GGA band gap's underestimation, we have used Engel-Vosko generalized gradient approximation (EVGGA),<sup>34</sup> which optimizes the corresponding potential for electronic band structure calculations. The Kohn-Sham equations are solved using a basis of linear APWs. The potential and charge density in the muffin-tin (MT) spheres are expanded in spherical harmonics with  $l_{max}=8$  and nonspherical components up to  $l_{max}=6$ . In the interstitial region, the potential and the charge density are represented by Fourier series. Self-consistency is obtained using 5000  $k$  points in the irreducible Brillouin zone (IBZ). We have calculated the transport properties using 11 560  $k$  points in the IBZ. The convergence of the total energy in the self-consistent

calculations is taken with respect to the total charge of the system with a tolerance 0.0001 electron charges. We have used the semi-classical Boltzmann theory as incorporated in BoltzTraP code<sup>30</sup> to calculate the thermoelectric properties like carrier concentration ( $n$ ), Seebeck coefficient ( $S$ ), electrical conductivity ( $\sigma/\tau$ ), electronic thermal conductivity ( $\kappa_e$ ), and the electronic power factor ( $S^2\sigma/\tau$ ) as a function of chemical potential at two constant temperatures (300 and 600) K. The constant relaxation time approximation and the rigid band approximation were used in the calculations.<sup>30</sup> BoltzTrap code depends on a well tested smoothed Fourier interpolation to obtain an analytical expression of bands. This is based on the fact that the electrons contributing to transport are in a narrow energy range due to the delta-function like Fermi broadening. For such a narrow energy range, the relaxation time is nearly the same for the electrons. The accuracy of this method has been well tested earlier, and the method actually turns out to be a good approximation.<sup>30,35–38</sup> The temperature dependence of the energy band structure is ignored. The formula of the transport coefficients as a function of temperature and chemical potential is given somewhere else.<sup>30,39</sup> To gain high thermoelectric efficiency, it is important that the material possesses high electrical conductivity, large Seebeck coefficient, and low thermal conductivity.<sup>40</sup>

## III. RESULTS AND DISCUSSION

### A. Salient features of the electronic band structures

The reliable transport properties can be obtained from accurately calculated electronic structure. Since the electronic band structure is the keynote factor for calculating the

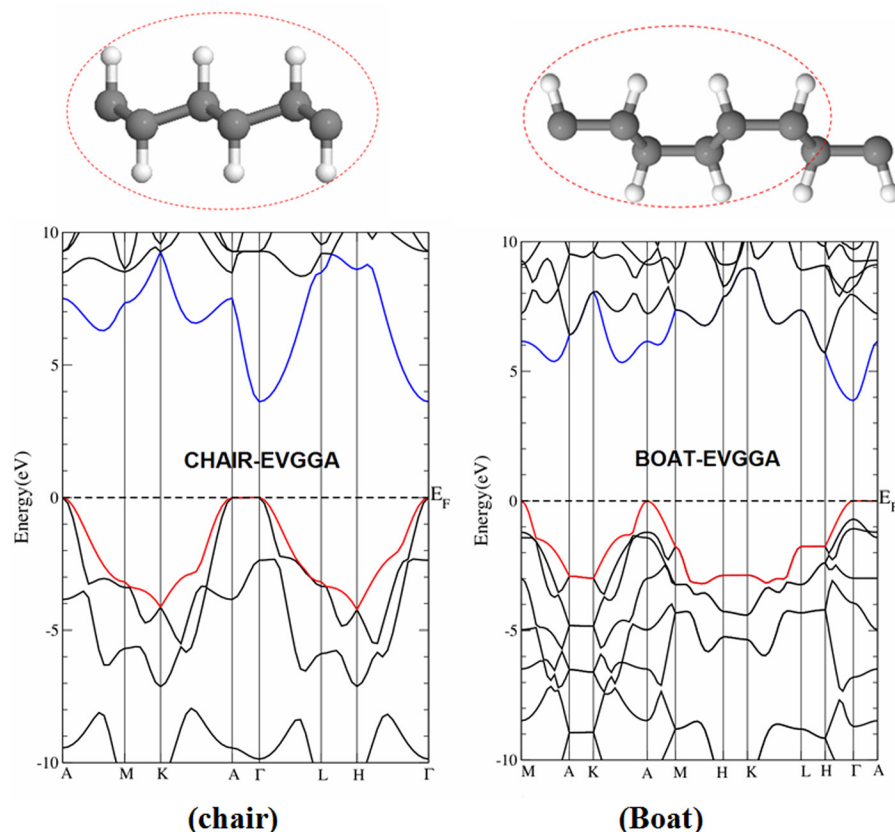


FIG. 1. The calculated electronic band structure for chair-like and boat-like graphane, the conduction band maximum is highlighted by red color and the valence band minimum by blue color just for identification. The chair-like conformer has  $P-3m1$  (trigonal) space group with unit cell  $a=2.516 \text{ \AA}$ ,  $b=2.516 \text{ \AA}$ , and  $c=4.978 \text{ \AA}$ , whereas the boat-like conformer has  $Pmnm$  (orthorhombic) space group with unit cell  $a=4.272 \text{ \AA}$ ,  $b=2.505 \text{ \AA}$ , and  $c=4.976 \text{ \AA}$ . Therefore, different high-symmetry points in the Brillouin zone (BZ) of chair-like conformer ( $P-3m1$  trigonal space group) than the boat-like conformer ( $Pmnm$  orthorhombic space group).

transport properties of the materials, thus let us recall the main features of the electronic band structure of chair-like and boat-like graphane. The electronic band structure along the high symmetry directions for the chair-like and boat-like graphane is shown in Fig. 1. It is clear that for both configurations the conduction band minimum (CBM) and the valence band maximum (VBM) are located at  $\Gamma$  point the center of the Brillouin zone (BZ), resulting in a direct band gap. The values of the energy gaps are 2.69 (3.02) eV using LDA, 3.02 (3.37) eV for GGA, and 3.60 (3.90) eV using EVGGA for chair-like (boat-like). To the best of our knowledge, there are no experimental data for the energy band gaps available in the literature to make a meaningful comparison. However, we can compare our calculated energy gaps using EVGGA with the previous theoretical calculations 3.49 eV (Ref. 26) and 3.50 eV (Ref. 25) for chair-like and 3.37 eV (Ref. 26) and 3.70 eV (Ref. 25) for boat-like, which show reasonable agreement. Future experimental work will testify our calculated results. This is mainly due to the fact that LDA and GGA have simple forms that are not sufficiently flexible to accurately reproduce both the exchange-correlation energy and its charge derivative. Engel and Vosko considered this shortcoming and constructed a new functional form of GGA that is able to better reproduce the exchange potential at the expense of less agreement in the exchange energy. Thus, EVGGA yields better band splitting and some other properties that mainly depend on the accuracy of the exchange-correlation potential. Therefore, we have decided to show the results obtained by EVGGA.

## B. Transport properties

### 1. Electrical conductivity

Increasing the temperature of the materials cause to increase the kinetic energy of the electrons. This lead to immigrate the electrons to the cold side resulting in an electric current. In order to have the highest electrical conductivity, high mobility carriers are required. The electrical conductivity ( $\sigma = ne\mu$ ) is directly proportional to the charge carriers density ( $n$ ) and their mobility ( $\mu$ ), where ( $\mu_e = e\tau_e/m_e^*$  and

$\mu_p = p\tau_p/m_p^*$ ) materials with small effective masses possess high mobility. The total carrier concentration is defined as the difference between the hole and the electron concentration. The electron and holes carrier concentration are defined as<sup>41</sup>

$$p = \frac{2}{\Omega} \int_{BZ} \int_{VB} [1 - f_0(T, \varepsilon, \mu)] D_v(\varepsilon) d\varepsilon, \quad (1)$$

$$e = \frac{2}{\Omega} \int_{BZ} \int_{CB} f_0(T, \varepsilon, \mu) D_c(\varepsilon) d\varepsilon. \quad (2)$$

In the above equation, the integral is performed over the BZ as well as over conduction band (CB) for electrons ( $e$ ) or valence band (VB) for holes ( $p$ ) and  $\Omega$  is the volume of unit cell, where  $D_v(\varepsilon)$  and  $D_c(\varepsilon)$  are the density of states of the valence and the conduction bands.

The charge carriers concentration of chair-/boat-like graphane as a function of temperature is illustrated in Fig. 2(a). It is clear that the charge carrier concentration linearly increases with increasing the temperature in agreement with the experimental work for graphene.<sup>42</sup> That means both configurations of the fully hydrogenated graphene (graphane) kept the same trend as the graphene. Chair-like graphane exhibits the highest carrier concentration along the temperature scale. The carrier concentration of chair (boat)-like graphane is about 0.0075 (0.007) e/uc at 600 K and 0.00065 (0.0003) e/uc at 50 K.

Fig. 2(b) illustrated the electrical conductivity of chair-like and boat-like graphane as a function of temperatures for fixed chemical potential. It is clear that the electrical conductivity increases linearly with increasing the temperatures<sup>43</sup> in agreement with the earlier theoretical work by Hwang and Das Sarma<sup>44</sup> and the experimental work of Efetov and Kim<sup>42</sup> for graphene. As the temperature increases,  $\sigma/\tau$  rapidly increases. The relaxation time is taken to be direction independent and isotropic.<sup>45</sup> The maximum value of electrical conductivity of chair (boat)-like graphane is about  $1.4 (0.6) \times 10^{19} (\Omega\text{ms})^{-1}$  at 600 K, while it is  $0.08(0.04) \times 10^{19} (\Omega\text{ms})^{-1}$  at 50 K.

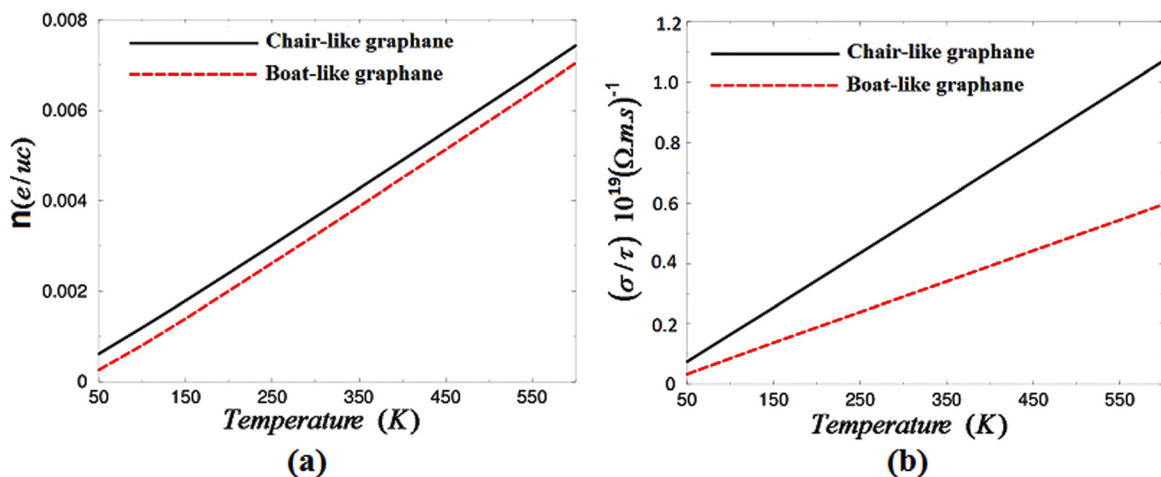


FIG. 2. (a) The calculated carrier concentration as a function of temperature for chair-like and boat-like graphane. (b) The calculated electrical conductivity as a function of temperature for chair-like and boat-like graphane.

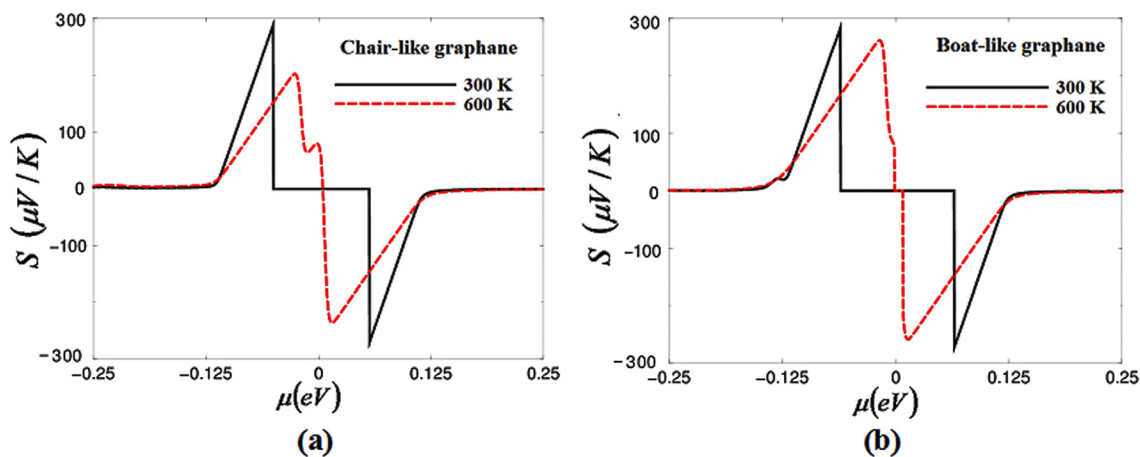


FIG. 3. The calculated Seebeck coefficient as a function of chemical potential at two constant temperatures 300 and 600 K for chair-like and boat-like graphane.

## 2. Seebeck coefficient

Seebeck coefficient ( $S$ ) or thermopower is related to the electronic structure of the materials. The sign of  $S$  indicates the type of dominant charge carrier, positive  $S$  represents the p-type materials, whereas n-type materials have negative  $S$ . The Seebeck coefficients of chair-like and boat-like vs chemical potential at 300 and 600 K are presented in Figs. 3(a) and

3(b). One can see in the vicinity of  $E_F$  that the Seebeck coefficient exhibits two pronounced peaks for n/p-type graphane. It has been found that these materials exhibit the highest value of Seebeck coefficient at 300 K of about 290 ( $\mu\text{V}/\text{K}$ ) and 280 ( $\mu\text{V}/\text{K}$ ) for p-type, while for n-type it is about 280 ( $\mu\text{V}/\text{K}$ ) and 270 ( $\mu\text{V}/\text{K}$ ) for chair-like and boat like, respectively. The critical points of Seebeck coefficient for p-type and n-type are  $-0.125$  and  $+0.125$   $\mu(\text{eV})$ , the range where

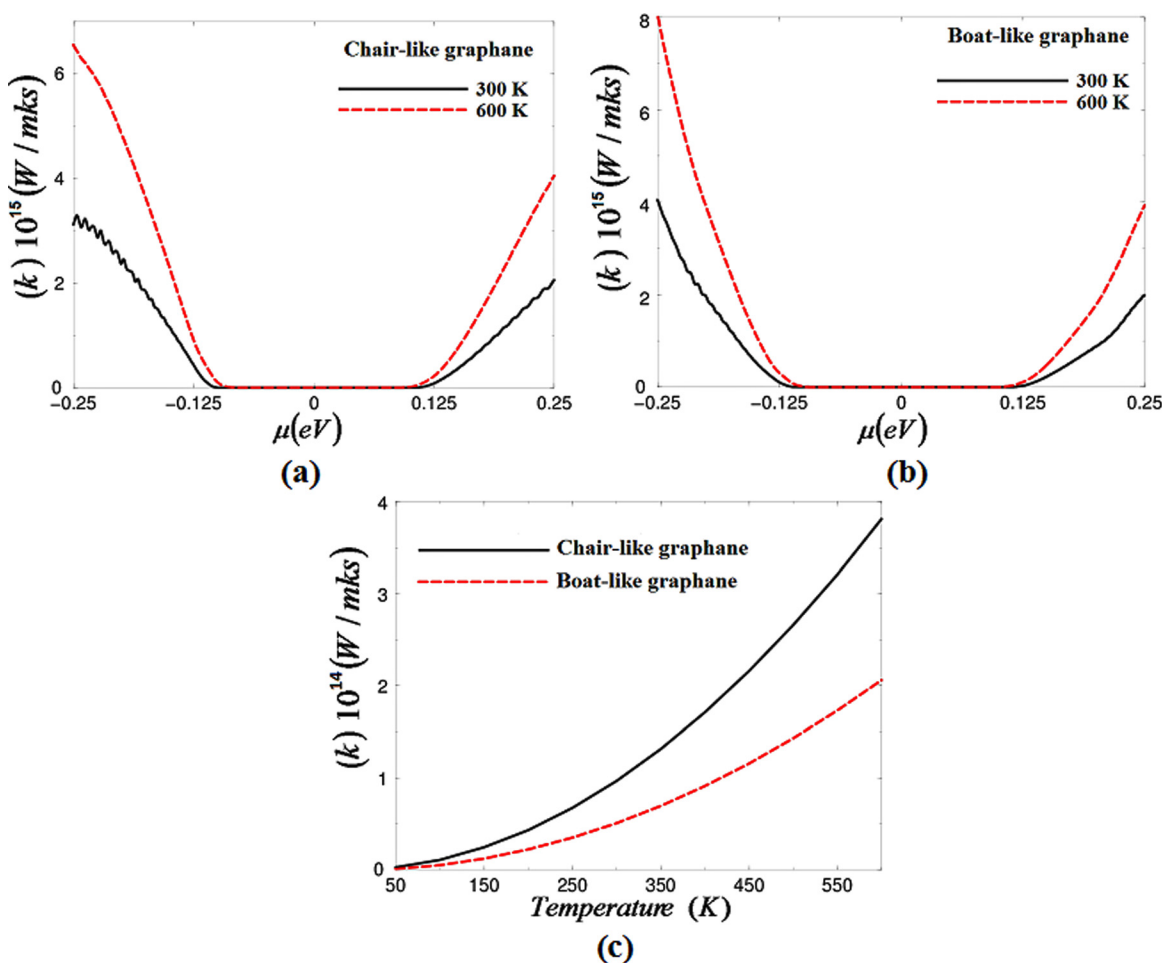


FIG. 4. (a) and (b) The calculated electronic thermal conductivity as a function of chemical potential at two constant temperatures 300 and 600 K for chair-like and boat-like graphane. (c) The calculated electronic thermal conductivity as a function of temperature for chair-like and boat-like graphane.

TABLE I. The maximum values of the electronic thermal conductivity at  $\pm 0.25 \mu\text{eV}$ .

Temperature	Chair-like graphane		Boat-like graphane	
	p-type ( $\times 10^{15}$ ) (W/Kms)	n-type ( $\times 10^{15}$ ) (W/Kms)	p-type ( $\times 10^{15}$ ) (W/Kms)	n-type ( $\times 10^{15}$ ) (W/Kms)
300 K	3.34	2.02	3.98	1.97
600 K	6.47	4.09	7.93	3.89

the materials exhibit good thermoelectric properties, and beyond this range the Seebeck coefficient is zero. We should emphasize that Wei *et al.*<sup>46</sup> experimentally observed that the Seebeck coefficient ( $S$ ) in graphene depends on the carrier density as  $n^{-\frac{1}{2}}$ , and shows a linear dependence with  $T$  at very low temperatures and the phonon drag contribution to the total  $S$  is a negligible.

### 3. Electronic thermal conductivity

For designing efficient thermoelectric devices, materials with low thermal conductivity are required in order to maintain the temperature gradient. The thermal conductivity ( $k = k_e + k_l$ ) consists of electronic (electrons and holes

transporting heat) and phonon (phonons traveling through the lattice) contributions, BoltzTraP calculates only the electronic part. The electronic thermal conductivity for chair-like and boat-like as a function of chemical potential for two different temperatures was presented in Figs. 4(a) and 4(b). We should emphasize that in the chemical potential between  $\mp 0.125 \mu\text{eV}$ , the investigated materials exhibit minimum value of thermal conductivity. Therefore,  $\mp 0.125 \mu\text{eV}$  is the region where chair-like and boat-like graphane is expected to give its maximum efficiency. The thermal conductivity values for p-type and n-type chair-like and boat-like at 300 and 600 K are presented in Table I, which show that the thermal conductivity of n-type has lower values than that of p-type.

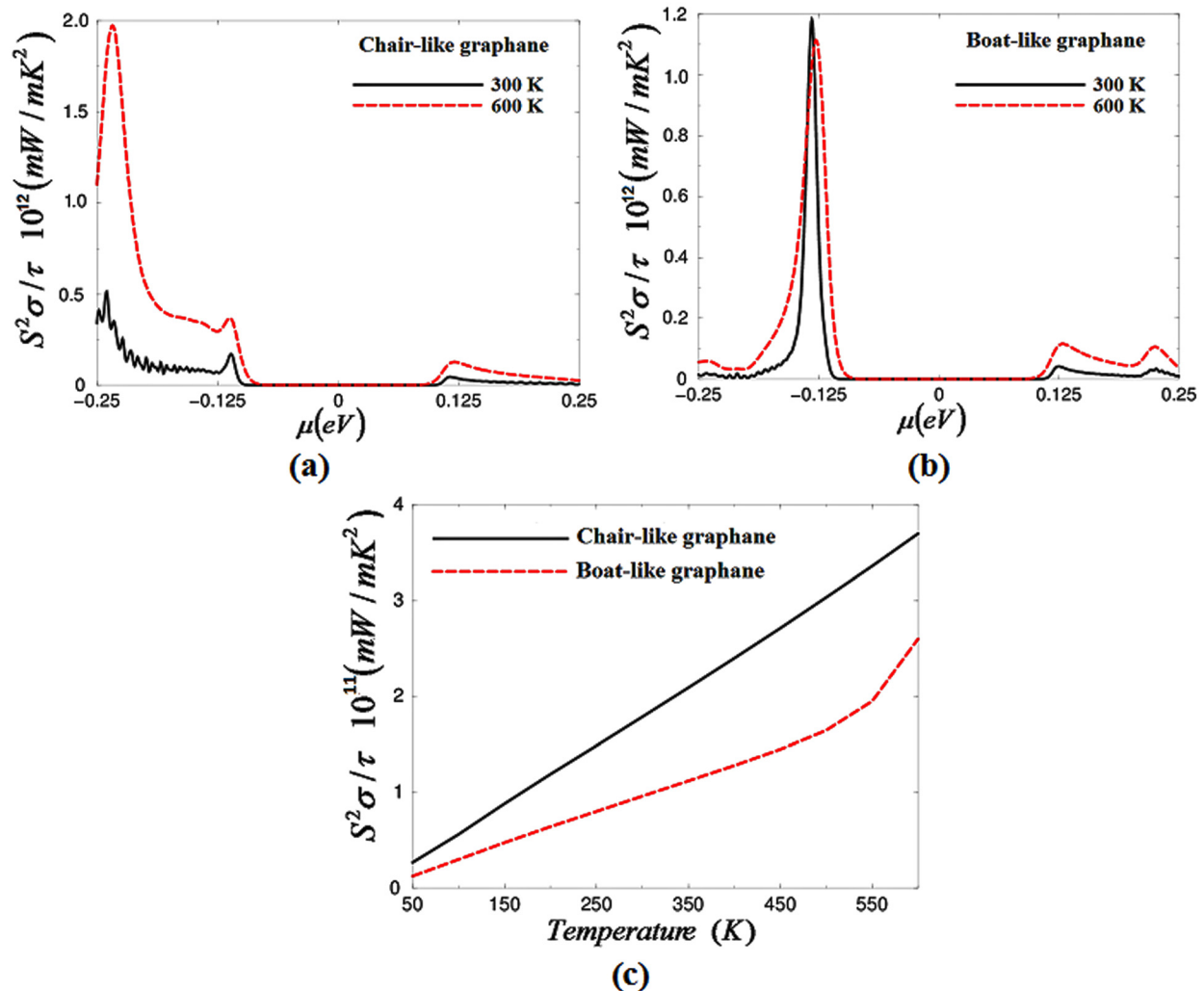


FIG. 5. (a) and (b) The calculated power factor as a function of chemical potential at two constant temperatures 300 and 600 K for chair-like and boat-like graphane. (c) The calculated power factor as a function of temperature for chair-like and boat-like graphane.

The thermal electronic conductivity of chair-like and boat-like graphane as a function of temperature is plotted in Fig. 4(c); it is clear that at low temperatures  $k_e$  is zero, as  $T$  increases the  $k_e$  increases exponentially in agreement with the experimental data of graphene.<sup>42</sup> The highest value of  $k_e$  for chair (boat)-like graphane of about  $3.5(2.0) \times 10^{14}$  (W/mKs) is achieved at 600 K.

#### 4. Power factor

Using the existence information on the Seebeck coefficient ( $S$ ) and the electrical conductivity ( $\sigma/\tau$ ), one can obtain the power factor ( $P = S^2\sigma/\tau$ ). It is clear that the power factor is directly proportional to Seebeck coefficient and electrical conductivity. The power factor comes as a numerator in the figure of merit relation ( $ZT = S^2\sigma T/\kappa$ ), therefore, it is very important quantity for calculating the transport properties of the materials. We have calculated the power factor of chair/boat-like graphane at 300 and 600 K as a function of chemical potential between  $\mp 0.25$   $\mu$ (eV) as illustrated in Figs. 5(a) and 5(b). At the vicinity of Fermi level, the power factor exhibits the minimum values that are attributed to fact that  $\sigma$  shows the minimum values in the vicinity of Fermi level and beyond that the power factor increases rapidly to form pronounced peak for p-type of chair-/boat-like graphane. The power factor of chair-like graphane exhibits a peak at around  $-0.24$   $\mu$ (eV), whereas for boat-like graphane the peak is situated at  $-0.126$   $\mu$ (eV) for both temperatures. In addition, we have calculated power factor of chair-/boat-like graphane vs temperature as shown in Fig. 5(c). We noticed that the power factor is linearly dependent on temperature. The highest values of power factor for chair (boat)-like graphane is about  $3.7(2.6) \times 10^{11}$  (mW/mK<sup>2</sup>) at 600 K and of about  $0.3(0.12) \times 10^{11}$  (mW/mK<sup>2</sup>) at 50 K.

#### IV. CONCLUSIONS

The state-of-the-art FPLAPW + lo method in a scalar relativistic version as embodied in the WIEN2k code was used to obtain accurately calculated electronic structure for chair-like and boat-like graphane (fully hydrogenated graphene). The electronic transport coefficients were evaluated by using the semi-classical Boltzmann theory and rigid band model. The charge carrier concentration and the electrical conductivity linearly increase with increasing the temperature in agreement with the experimental work for graphene. The highest values of the charge carrier concentration and the electrical conductivity are achieved at 600 K. The highest value of Seebeck coefficient is about 290 ( $\mu$ V/K) and 280 ( $\mu$ V/K) for p-type, while for n-type it is 280 ( $\mu$ V/K) and 270 ( $\mu$ V/K) for chair-like and boat like, respectively. These values were achieved at 300 K. We should emphasize that for the chemical potential between  $\mp 0.125$   $\mu$ (eV) the investigated materials exhibit minimum value of thermal conductivity. Therefore,  $\mp 0.125$   $\mu$ (eV) is the region where chair-like and boat-like graphane expected to give its maximum efficiency. The power factor of chair-/boat-like graphane at 300 and 600 K was calculated as a function of chemical potential between  $\mp 0.25$   $\mu$ (eV). The power factor of chair-like graphane exhibits a peak at around  $-0.24$   $\mu$ (eV),

whereas for boat-like graphane the peak is situated at  $-0.126$   $\mu$ (eV) for 300 and 600 K. The highest power factor occurs at 600 K, thereafter it decreases with decreasing the temperature.

#### ACKNOWLEDGMENTS

The result was developed within the CENTEM project, Reg. No. CZ.1.05/2.1.00/03.0088, cofunded by the ERDF as part of the Ministry of Education, Youth and Sports OP RDI programme and, in the follow-up sustainability stage, supported through CENTEM PLUS (LO1402) by financial means from the Ministry of Education, Youth and Sports under the "National Sustainability Programme I." Computational resources were provided by MetaCentrum (LM2010005) and CERIT-SC (CZ.1.05/3.2.00/08.0144) infrastructures.

- <sup>1</sup>H. Wang, W. Chu, and H. Jin, "Theoretical study on thermoelectric properties of Mg2Si and comparison to experiments," *Comput. Mater. Sci.* **60**, 224–230 (2012).
- <sup>2</sup>K. P. Ong, D. J. Singh, and P. Wu, "Analysis of the thermoelectric properties of *n*-type ZnO," *Phys. Rev. B* **83**, 115110 (2011).
- <sup>3</sup>D. Parker and D. J. Singh, "Transport properties of hole-doped CuBiS2," *Phys. Rev. B* **83**, 233206 (2011).
- <sup>4</sup>D. Parker, M.-H. Du, and D. J. Singh, "Doping dependence of thermoelectric performance in Mo3Sb7: First-principles calculations," *Phys. Rev. B* **83**, 245111 (2011).
- <sup>5</sup>D. J. Singh, "Doping-dependent thermopower of PbTe from Boltzmann transport calculations," *Phys. Rev. B* **81**, 195217 (2010).
- <sup>6</sup>K. P. Ong, D. J. Singh, and P. Wu, "Unusual transport and strongly anisotropic thermopower in PtCoO2 and PdCoO2," *Phys. Rev. Lett.* **104**, 176601 (2010).
- <sup>7</sup>G. B. Wilson-Short, D. J. Singh, M. Fornari, and M. Suewattana, "Thermoelectric properties of rhodates: Layered  $\beta$ -SrRh2O4 and spinel ZnRh2O4," *Phys. Rev. B* **75**, 035121 (2007).
- <sup>8</sup>D. J. Singh and D. Kasinathan, "Thermoelectric properties of NaxCoO2 and prospects for other oxide thermoelectrics," *J. Electron. Mater.* **36**, 736 (2007).
- <sup>9</sup>D. J. Singh, "Electronic and thermoelectric properties of CuCoO2: Density functional calculations," *Phys. Rev. B* **76**, 085110 (2007).
- <sup>10</sup>D. J. Singh, "Oxide thermoelectrics," *MRS Proc.* **1044**, 1044-U02-05 (2007).
- <sup>11</sup>D. J. Singh, "Alkaline earth filled nickel skutterudite antimonide thermoelectrics," U.S. patent 8,487,178 (16 July 2013).
- <sup>12</sup>J. Seol, I. Jo, A. Moore, L. Lindsay, Z. Aitken, M. Pettes, X. Li, Z. Yao, R. Huang, D. Broido, N. Mingo, R. Ruoff, and L. Shi, "Two-dimensional phonon transport in supported graphene," *Science* **328**, 213 (2010).
- <sup>13</sup>Y. Zuev, W. Chang, and P. Kim, "Thermoelectric and magnetothermoelectric transport measurements of graphene," *Phys. Rev. Lett.* **102**, 96807 (2009).
- <sup>14</sup>C. Palma and P. Samor, "Blueprinting macromolecular electronics," *Nat. Chem.* **3**, 431 (2011).
- <sup>15</sup>H. Sevincli and G. Cuniberti, "Enhanced thermoelectric figure of merit in edge-disordered zigzag graphene nanoribbons," *Phys. Rev. B* **81**, 113401 (2010).
- <sup>16</sup>Y. Lu, B. R. Goldsmith, N. J. Kybert, and A. T. C. Johnson, "DNA-decorated graphene chemical sensors," *Appl. Phys. Lett.* **97**, 083107 (2010).
- <sup>17</sup>Z. M. Ao, J. Yang, S. Li, and Q. Jiang, "Enhancement of CO detection in Al doped graphene," *Chem. Phys. Lett.* **461**, 276 (2008).
- <sup>18</sup>O. Leenaerts, B. Partoens, and F. M. Peeters, "Adsorption of H2O, NH3, CO, NO2, and NO on graphene: A first-principles study," *Phys. Rev. B* **77**, 125416 (2008).
- <sup>19</sup>H. J. Yoon, D. H. Jun, J. H. Yang, Z. Zhou, S. S. Yang, and M. M.-C. Cheng, "Carbon dioxide gas sensor using a graphene sheet," *Sens. Actuators, B* **157**, 310 (2011).
- <sup>20</sup>A. K. Manna and S. K. Pati, "Tuning the electronic structure of graphene by molecular charge transfer: A computational study," *Chem. Asian J.* **4**, 855 (2009).

- <sup>21</sup>W. Chen, S. Chen, D. C. Qi, X. Y. Gao, and A. T. S. Wee, "Surface transfer p-type doping of epitaxial graphene," *J. Am. Chem. Soc.* **129**, 10418 (2007).
- <sup>22</sup>S. Gowtham, R. H. Scheicher, R. Ahuja, R. Pandey, and S. P. Karna, "Physisorption of nucleobases on graphene: Density-functional calculations," *Phys. Rev. B* **76**, 033401 (2007).
- <sup>23</sup>M. H. F. Sluiter and Y. Kawazoe, "Cluster expansion method for adsorption: Application to hydrogen chemisorption on graphene," *Phys. Rev. B* **68**, 085410 (2003).
- <sup>24</sup>D. C. Elias, R. R. Nair, T. M. G. Mohiuddin, S. V. Morozov, P. Blake, M. P. Halsall, A. C. Ferrari, D. W. Boukhvalov, M. I. Katsnelson, A. K. Geim, and K. S. Novoselov, "Control of graphene's properties by reversible hydrogenation: Evidence for graphane," *Science* **323**, 610 (2009).
- <sup>25</sup>J. O. Sofo, A. S. Chaudhari, and G. D. Barber, "Graphane: A two-dimensional hydrocarbon," *Phys. Rev. B* **75**, 153401 (2007).
- <sup>26</sup>C. He, C. X. Zhang, L. Z. Sun, N. Jiao, K. W. Zhang, and J. Zhong, "Structure, stability and electronic properties of tricycle type graphane," *Phys. Status Solidi RRL* **6**(11), 427–429 (2012).
- <sup>27</sup>F. Karlicky, R. Zboril, and M. Otyepka, "Band gaps and structural properties of graphene halides and their derivatives: A hybrid functional study with localized orbital basis sets," *J. Chem. Phys.* **137**(3), 034709 (2012).
- <sup>28</sup>F. Karlicky and M. Otyepka, "Band gaps and optical spectra of chlorographene, fluorographene and graphane from G<sub>0</sub>W<sub>0</sub>, GW<sub>0</sub> and GW calculations on top of PBE and HSE06 orbitals," *J. Chem. Theory Comput.* **9**(9), 4155–4164 (2013).
- <sup>29</sup>X. Ni, G. Liang, J.-S. Wang, and B. Li, "Disorder enhances thermoelectric figure of merit in armchair graphane nanoribbons," *Appl. Phys. Lett.* **95**, 192114 (2009).
- <sup>30</sup>G. K. H. Madsen and D. J. Singh, "BoltzTraP. A code for calculating band-structure dependent quantities," *Comput. Phys. Commun.* **175**, 67–71 (2006).
- <sup>31</sup>P. Blaha, K. Schwarz, G. K. H. Madsen, D. Kvasnicka, and J. Luitz, *WIEN2k, An Augmented Plane Wave Plus Local Orbitals Program for Calculating Crystal Properties* (Vienna University of Technology, Austria, 2001).
- <sup>32</sup>J. P. Perdew, S. Burke, and M. Ernzerhof, "Generalized gradient approximation made simple," *Phys. Rev. Lett.* **77**, 3865 (1996).
- <sup>33</sup>D. M. Ceperley and B. I. Aker, *Phys. Rev. Lett.* **45**, 566–569 (1980); parametrized in J. P. Perdew and A. Zunger, *Phys. Rev. B* **8**, 4822–4832 (1973).
- <sup>34</sup>E. Engel and S. H. Vosko, "Exact exchange-only potentials and the virial relation as microscopic criteria for generalized gradient approximations," *Phys. Rev. B* **47**, 13164 (1993).
- <sup>35</sup>R. Chmielowski, D. Pere, C. Bera, I. Opahle, W. Xie, S. Jacob, F. Capet, P. Roussel, A. Weidenkaff, G. K. H. Madsen, and G. Dennler, *J. Appl. Phys.* **117**, 125103 (2015).
- <sup>36</sup>H. Shi, D. Parker, M.-H. Du, and D. J. Singh, *Phys. Rev. Appl.* **3**, 014004 (2015).
- <sup>37</sup>G. Dennler, R. Chmielowski, S. Jacob, F. Capet, P. Roussel, S. Zastrow, K. Nielsch, I. Opahle, and G. K. H. Madsen, *Adv. Energy Mater.* **4**, 1301581 (2014).
- <sup>38</sup>D. Wang, L. Tang, M. Q. Long, and Z. G. Shuai, *J. Chem. Phys.* **131**, 224704 (2009).
- <sup>39</sup>T. J. Scheidemantel, C. Ambrosch-Draxl, T. Thonhauser, J. V. Badding, and J. O. Sofo, "Transport coefficients from first-principles calculations," *Phys. Rev. B* **68**, 125210 (2003).
- <sup>40</sup>G. J. Snyder and E. S. Toberer, "Complex thermoelectric materials," *Nature Mater.* **7**, 105–114 (2008).
- <sup>41</sup>C. C. Hu, "Electrons and holes in semiconductors," in *Modern Semiconductor Devices for Integrated Circuits* (Pearson/Prentice Hall, 2011), Part I, p. 11.
- <sup>42</sup>D. K. Efetov and P. Kim, *Phys. Rev. Lett.* **105**, 256805 (2010).
- <sup>43</sup>E. Murioz, *J. Phys.: Condens. Matter* **24**, 195302 (2012).
- <sup>44</sup>E. H. Hwang and S. Das Sarma, *Phys. Rev. B* **77**, 115449 (2008).
- <sup>45</sup>B. Xu, X. Li, G. Yu, J. Zhang, S. Ma, Y. Wang, and L. Yi, *J. Alloys Compd.* **565**, 22–28 (2013).
- <sup>46</sup>P. Wei, W. Bao, Y. Pu, C. N. Lau, and J. Shi, *Phys. Rev. Lett.* **102**, 166808 (2009).